Terrain Classification and Locomotion Parameters Adaptation for Humanoid Robots Using Force/Torque Sensing

Krzysztof Walas[1], Dimitrios Kanoulas[2], and Przemyslaw Kryczka[2]

***Abstract*— This paper describes a terrain classification method based on the readings from the force/torque sensors mounted on the ankles of a humanoid robot. The experimental results on five different terrain types, showed very high precision and recall identification rates, i.e. 95%, that are surpassing the state-of-the-art ones for quadrupeds and hexapods. Based on the acquired data during a set of walking experiments, we evaluated the stability of locomotion on all of the terrains. We also present a method to find an optimal step size, which optimises both the energy consumption and the stability of locomotion, given the identified terrain type. For the experimental data collection we used the full-size humanoid robot WALK-MAN walking on five different types of terrain.**

I. INTRODUCTION

Research on humanoid robots has its long history with several waves of interest in the topic. Over the past few years we observed a renaissance in the research on bipedal locomotion. This is due to the 2015 DARPA Robotics Challenge (DRC), where humanoid robots were supposed to perform in scenarios related to disaster response tasks. One of the observations, according to the report in [1], is that the robots' behaviour in the DRC was fragile. This remark is followed by the suggestion that the ways to make robots robust, even under expected variations, are sought. In this paper we are presenting a step towards this goal. Through terrain perception we allow the robot to accommodate its locomotion to the variation of the terrain parameters.

The importance of the investigated problem lays in the fact that in most of the bipedal locomotion approaches, hard contacts with the ground are assumed. Whereas, in real life scenarios this may not be true. Even though there is a margin (allowed error) in the locomotion controller that makes the robot compliant to the small terrain variations [2], there are no explicit implementations which deal with the changing terrain properties. This negligence may lead to the catastrophic consequence of falling down while walking on an unmodeled terrain. In such a scenario the robot may be unable to continue its mission. Having an algorithm that allows the robot to identify the terrain with high confidence, using the sensors on its feet, will give the possibility to eliminate most of the falls while walking on different surfaces.

[1]Krzysztof Walas is with the Institute of Control and Information Engineering, Poznan University of Technology, Poznan, Poland. krzysztof.walas@put.poznan.pl

[2]Dimitrios Kanoulas and Przemyslaw Kryczka are with the Department of Advanced Robotics, Istituto Italiano di Tecnologia (IIT), Via Morego 30, 16163, Genova, Italy. {Dimitrios.Kanoulas, Przemyslaw.Kryczka}@iit.it

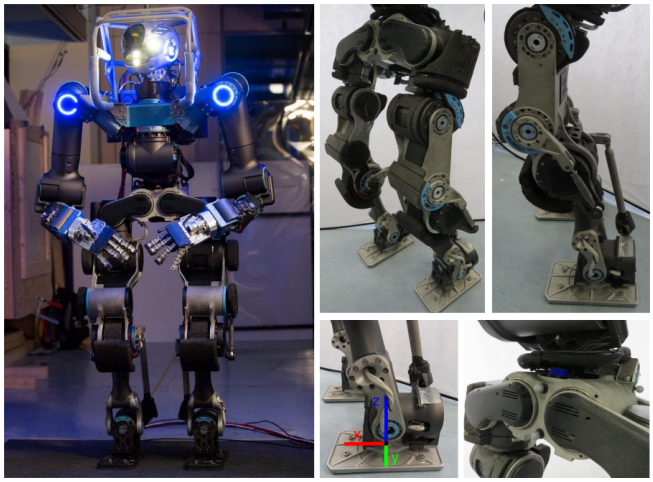

Fig. 1. The full-size humanoid robot WALK-MAN. In detail: the legs, the foot, the ankle-mounted force/torque sensor (with its local axes), and the pelvis including the Inertial Measurement Unit (IMU) in blue.

A. State of the Art

In our survey of the related work we first focus on the humanoid robots and their locomotion controllers and then present different approaches to tactile terrain perception for multi-legged robotic platforms. We end the review with some examples of using different sensing modalities for terrain identification.

a) Humanoid Robots: The gait control system for the contemporary humanoid robots is mostly based on the Zero Moment Point (ZMP) computation. Robots such as STARO [3], Valkyrie [4], and WALK-MAN [5] are using such an approach together with motor position control. The reference positions of the joints come from the locomotion controller, which in many cases is based on a Linear Inverted Pendulum (LIP) model, e.g. the preview controller developed by Kajita et al. [6], which is used in HUBO [7], HRP-2 [8], and many other robots. Kuindersma et al. [9] extended this approach to a continuous time-varying linear-quadratic regulator problem for ZMP tracking and applied it to the ATLAS robot. The controllers that were used in the aforementioned robots do not model ground properties. A robot which is explicitly addressing this issue in its control algorithm is THORMANG [10], where mass-spring-damper model of contact is used. Another similar controller was developed by Hashimoto et al. [11], where a mass-spring model of the terrain was used. The ankle orientation was controlled to enable their robot, WABIAN-2R, to walk on a

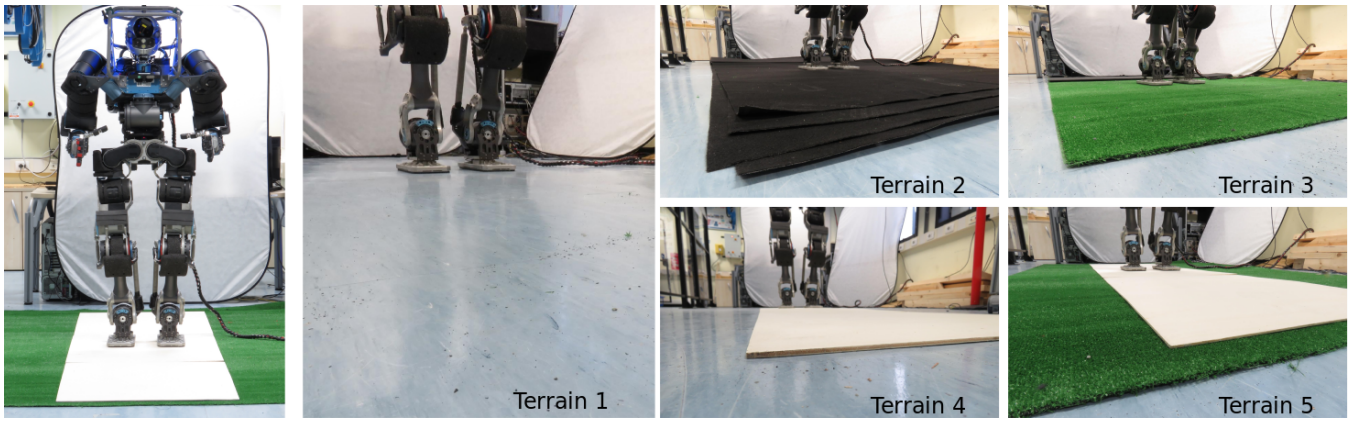

Fig. 2. **Left:** The robot on the fifth terrain type (thin wood on the grass carpet). **Right:** The five experimental terrain types.

soft terrain. In the approach implemented on the ESCHER robot [2], the locomotion on soft terrains is enabled by empirically shifting the Center-of-Pressure (CoP) towards the inner part of the supporting feet, while skipping the terrain modelling. Brandao et al. [12] proposed a method to optimise the gait parameters depending on the frictional properties of the terrain, while a bio-inspired foothold selection system for bipeds was introduced in [13], [14]. In most of the existing methods, however, the terrain is either identified in advance or is assumed to be known, while the terrain identification problem is not being addressed.

b) Tactile Terrain Identification: Although, the problem of perception for terrain identification has not been extensively explored so far in the literature for humanoid robots, a lot of work has been done for other types of legged platforms. In one of the latest examples in [15], the quadruped robot AIBO was able to distinguish six indoor surface types, using the fused accelerometer and ground contact force sensor data. An interesting research work, related to our contribution, was described in [16]. In that work, a quadruped robot was traversing different grounds using a variety of gaits. Based on a proprioceptive suit of sensors (encoders on active and passive compliant joints), inertial units, and foot pressure sensors, the influence of different gaits on classification performance was assessed. In [17], a technically blind six-legged walking robot, was able to identify terrains, using feedback from the robot's actuators and the desired trajectory.

Most of the work on terrain classification is done using various approaches of supervised learning. However, in [18] the authors performed unsupervised tactile data clustering, using the Pitman-Yor process. Additionally, in [19] a ground model identification framework was presented, where experiments were performed for a single leg in a very controlled environment and the relationship between the parameters of the conventional models and the terramechanics models were found.

c) Terrain Identification with other Sensing Modalities: To show our results in a broader scope, some of the terrain identification examples, using different sensing modalities, are given. Vision was used for terrain identification in the task of quadruped locomotion [20], while the use of a 7 bend spectral camera together with the visual light bands was proposed in [21]. In addition, the use of Laser Range Finder, exploiting intensity signals, was described in [22].

B. Contribution

Encouraged by our previous achievements on tactile terrain identification for a six-legged robot [23] and other approaches for quadruped robots such as in [24], we have posited the hypothesis. It is possible to perform terrain identification and adjust gait parameters of a humanoid robot based on the tactile perception. The contribution of our work is threefold. First, we show that the tactile perception is a reliable source of information for terrain identification on humanoid robots. Additionally, we apply a new descriptor for force/torque signals to achieve a better classification performance than the state-of-the-art solutions ($\sim 8\%$ better in terms of precision and $\sim 5\%$ in terms of recall rate). Finally, we provide an example of how the gait parameters can be optimised, based on the terrain type that was identified in the classification process and the locomotion performance on each terrain in terms of energy and stability.

The structure of the paper is as follows. First, the robotic platform and the experimental setup are presented. Next, the tactile perception and the terrain classification methods are described, followed by the methodology of gait parameters optimisation based on the robot energy expenditure and the locomotion stability. Subsequently, the classification and stability/energy results are provided, followed by the conclusions and the future work plans.

II. Setup

In this section, we first describe the robotic system along with its locomotion controller, and then present the flat terrain types that were used for the classification and the locomotion energy/stability analysis.

A. Robot Description

For the experimental demonstration of the introduced method, we use the full-size humanoid robot WALK-MAN

(Fig. 1). WALK-MAN is an electric motor driven robot with 31 Degrees-of-Freedom (DoF). In the experiments only the legs (6DoF each) and the pelvis have been used for locomotion. The robot is 1.91m tall and weighs 118kg (without the battery). Its Series Elastic high-end Actuation (SEA) units can reach velocities up to 19.5rad/sec and torques up to 400Nm. There are four 6DoF force/torque (F/T) sensors at the end-effectors, two at the wrists and two at the ankles. The local coordinate frame of the ankle's F/T sensor, which was used in this paper, is attached to each robot's foot in the way that is shown in the lower part of Fig. 1. An Inertial Measurement Unit (IMU) is attached at the pelvis to record the acceleration and orientation state, while the visual sensor is a CMU Multisense-SL system which includes a stereo camera, a lidar sensor, and an IMU. For the communication, we use the YARP middleware framework [25], while the visual and the force/torque data are acquired using the ROS [26] framework.

1) Locomotion Control: To move the robot, we use a motor position controller. The joint space references are the result of the precomputed gait pattern and the real-time feedback controller. The gait pattern is a set of task space references that fully define the 3D motion of the robot in space. For the purpose of pure locomotion we use the references of the pelvis and the feet, and freeze the upper body at a chosen configuration.

The trajectory of the pelvis is generated based on the reference trajectories of the end-effectors and the ZMP, which depend on the step size and its duration. It is calculated with the preview controller developed by Kajita et al. [6], which in the first iteration generates the initial Center-of-Mass (CoM) trajectory and then simulates the motion using a multibody model of the robot to calculate the expected ZMP trajectory. Then, the discrepancy between the initial ZMP reference and the ZMP from the multibody model simulation is used to modify the CoM reference to improve the ZMP tracking. Finally, the CoM reference is translated into the pelvis reference at every sampling time of the multi-body simulation.

When the gait pattern is executed in the feed-forward manner, the errors in the modelling and environment reconstruction can cause an unstable locomotion, especially on the WALK-MAN platform equipped with SEAs. To stabilise the locomotion we use the torso position compliance controller that was introduced in [27]. The controller, based on the estimated ZMP position, modifies the pelvis reference to simultaneously track the ZMP reference and prevent the divergence of the CoM from the original reference.

B. Apparatus Setup

The experimental setup involves the following five types of terrain, for which the locomotion varies in stability due to difference in their properties, such as stiffness and friction (Fig. 2):

- terrain 1: a solid ground floor
- terrain 2: a 4-layers black carpet
- terrain 3: a single layer grass carpet

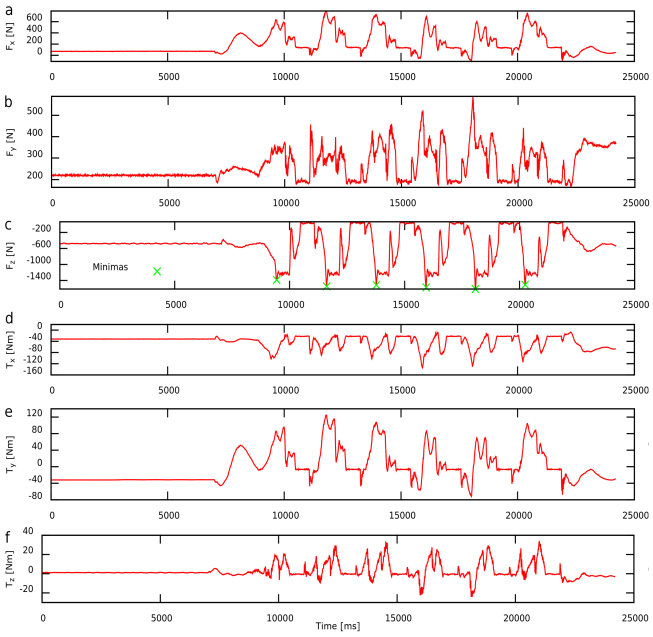

Fig. 3. An example of measured force and torque signals, with the sensor mounted on the left ankle. The robot was walking on a solid ground (i.e. terrain 1) with a $10cm$ step length. Each subplot represents a different signal.

- terrain 4: a layer of thin wood on the solid ground floor
- terrain 5: a layer of thin wood on the grass carpet

The 4-layers black carpet is totally 6.5mm thick, while the thickness of the grass carpet and the wood is 5.3mm and 4.5mm, respectively. In every experimental run we set the robot on each of the five flat terrains and we let it walk 10 steps ahead, remaining solely on the same terrain type. For each terrain we run 5 experiments, by changing the locomotion step size to 0.02m, 0.04m, 0.06m, 0.08m, and 0.1m, respectively. We run each of these experiments 5 times, 50 steps per each terrain and stride size. For all the terrains we gathered 1250 steps in total. Note that each step is planned to be executed in 1.3sec independent of the step size.

For each trial we collected the following data: the ankle force/torque measurements for each leg at 100Hz and the pelvis IMU data including orientation and acceleration at 200Hz.

III. Methods

Having described the robotic system and the terrain types, we now present the data acquisition and processing procedure, followed by the terrain classification method and the energy/stability analysis that was used for the gait parameter adaptation.

A. Tactile Perception

The terrain identification is based on the registered ankle F/T data. A sample reading from the left F/T ankle sensor, while the robot is walking on the solid ground floor with a 10 cm step length, is shown in Fig. 3. Each of the subplots

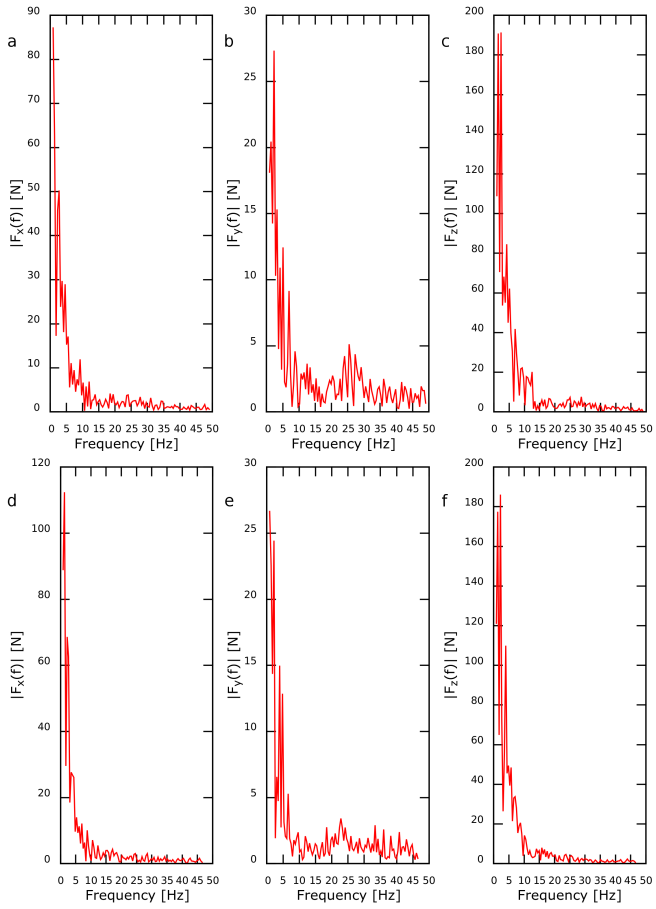

Fig. 4. Fourier responses for two different terrain types: the solid ground (terrain 1) and the thin wood on the grass carpet (terrain 5). The robot step size equals to 10cm. Subplots (a) and (d) show the spectrum for the F_x signals, (b) and (e) for the F_y, and (c) and (f) for the F_z data accordingly.

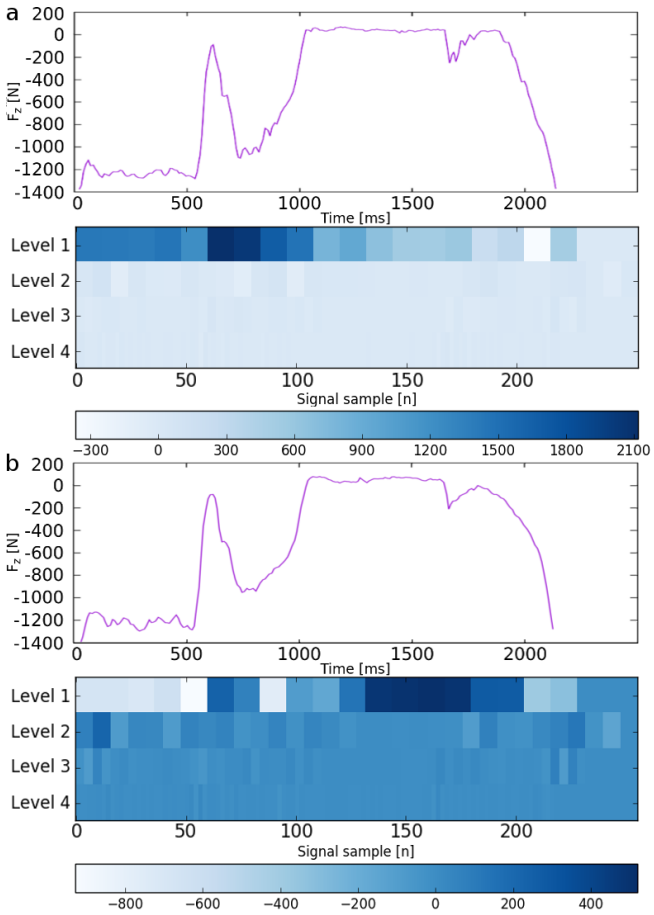

Fig. 5. Discrete Wavelet Transform responses for two different terrain types: the solid ground (terrain 1) and the thin wood on the grass carpet (terrain 5). The robot step size equals to 10 cm. The scalogram for the F_z signal recorded for terrain 1 (a) and for terrain 5 (b).

presents different force or torque signals. The recorded signals for each experimental trial include 5 steps for both left and right leg, i.e. 10 steps in total. Such data require further processing. The recorded signals were split into separate steps. Based on the F_z signal reading, we search for its local minima – impacts when the foot is touching the ground. A set of samples that starts in one minimum and ends in the subsequent one is treated as a single step. An example result of this procedure is marked with green crosses, as illustrated in Fig. 3-c.

B. Terrain Classification

Using the single steps that were extracted as described in Sec. III-A, we computed the descriptors of the signals. In our approach two methods were used for data reduction: the Fast Fourier Transform (FFT) and the Discrete Wavelet Transform (DWT). The FFT approach was successfully applied for a similar problem in our previous work in [23], while the DWT, to the best of our knowledge, is applied for the first time in a terrain classification process based on F/T signals.

First, we used and focused on the FFT approach. An example output of the FFT for the force signals is shown in Fig. 4. The vector of features is built using 20 modes from the spectrum (2–21). The exclusion of the first mode, which is mostly dominating and suppressing the information content from the subsequent modes with smaller responses, is intentional. In [23] we presented more details and tests on the appropriate number of samples and the arrangement of the window. The whole feature vector consists of 120 elements – 6 $signals \times 20$ $features$.

In our second approach we used the DWT method. The output of such a transformation is shown in Fig. 5. In our case the Daubechies wavelet [28], which is commonly used in the signal processing community, was used. Namely, the one with 4 vanishing moments (db4) was applied. In Fig. 5-a, the scalogram represents the responses of the scaled db4 on different levels, for the F_z signal that was recorded on the solid ground (terrain 1). In the DWT the mother wavelet is translated in the time domain (at a certain level) and dilated (stretched) in the frequency domain (level switch). The wavelet is localised in the time and frequency domains simultaneously, contrary to the FFT, where only localisation in the frequency domain is provided. The use of the DWT gives the advantage of having a richer descriptor of the signal, especially when the signal is non-stationary, which

is the case for the data recorded in our experiments. Fig. 5-b represents the scalogram obtained for a different terrain type, i.e. wood on grass carpet (terrain 5). The differences between scalograms in Fig. 5-a and Fig. 5-b could be visually observed. This gives the intuitive observation that this type of descriptor could provide good discrimination between terrain classes.

Let us now provide more details of the descriptor. The responses from level 1 and level 2 of the scalogram were used. As can be observed in Fig. 5, these two levels provide most of the variability in the responses and at the same time allow our feature vector to be reasonably short. This is due to the fact that we are taking wavelet responses for the coarsest scales. The first and the second level provides 17 and 28 responses, respectively. Therefore, the number of features for the DWT descriptor is equal to $(level1\ resp. + level2\ resp.) \times 6\ signals = (17+28) \times 6 = 270\ features$, comparing to $120\ features$ for FFT.

Having the feature vector for each step, the learning procedure was performed using Support Vector Machines (SVM) with C-Support Vector Classification and radial basis function of degree 3. The library that was used is the LIBSVM [29]. For each terrain type and a given robot step size, we used 30 steps for learning and 10 steps for testing. Given that we performed learning for all the five terrain types in our experiments, this sums up to 150 steps for learning and 50 steps for testing. Based on the knowledge about the influence of the speed of the movement on the classification process [16], [30] we have performed two types of experiments. In the first one, classification is performed separately for each step size. In the second one, all the steps are put into a large training and testing set. The outcome of these two approaches is described in the results section.

C. Locomotion Energy and Stability Analysis

Given the present control method of our robot, without a real-time gait regeneration or the ankle admittance controllers, the only parameter that we can control is the step length. The major factors that can quantify the locomotion performance are the energy cost and the stability of locomotion. These topics will be addressed in the following paragraphs.

1) Energy Expenditure: Since the robot's embedded joint torque sensors were not functional during the experiments and we also did not have an access to the motor current data, we performed the energy analysis in simulation (GAZEBO [31]). At this point, since the terrains were relatively thin, we assumed that the energy consumption due to different terrains will be negligible, compared to the energy consumption due to the locomotion time. We computed the total energy expenditure of the robot when it walks 0.5m with various step sizes $x \in A = \{0.02, 0.04, 0.06, 0.08, 0.1\}$m. To calculate the overall energy that is consumed for each step size we used the following formula:

$$\boldsymbol{e}_x = \sum_{i=1}^{n} |\boldsymbol{\tau}_i^T| \cdot |\Delta \boldsymbol{q}_i|, \quad for\ n = \frac{t_x}{\Delta t} \tag{1}$$

where, $\boldsymbol{\tau}$ is the vector containing all the joint torques, $\Delta \boldsymbol{q}$ is the joint space displacement, t_x is the duration of locomotion for the individual step length x and Δt is the sampling time. We performed the calculation for all the step sizes and obtained the following energy costs (expressed in J), from the shortest to the longest step size:

$$\boldsymbol{e} = [2507,\ 1328,\ 1084,\ 1062,\ 747]J \tag{2}$$

We can clearly notice that the energy expenditure decreases with the step size. This is expected, as the smaller the step size is, the longer it takes for the robot to reach the 0.5m goal.

2) Stability: To evaluate the locomotion stability, we should ideally compare the estimated CoM position and velocity to their references. However, the proper state estimator implemented was not available on the robot during experiments. Therefore, we focused on the analysis of an error between the measured ZMP position and its reference coming from the gait pattern generator. While performing experiments we noticed that the robot was much less stable when walking on terrains number: 3 (grass carpet) and 5 (wood on grass carpet). We verified the average ZMP error for different terrains, but we didn't manage to find any correlation between the error and the terrain type or the step size. Analysis of the standard deviation (SD) of the ZMP error has shown, however, a clear relation between the terrain type and the increase in the ZMP error variation, which confirms the visually observed stability degradation. Examples of the ZMP error standard deviation for terrains number 1 (solid ground) and 5 (wood on grass carpet) are presented in Fig. 6. We can notice a clear correlation

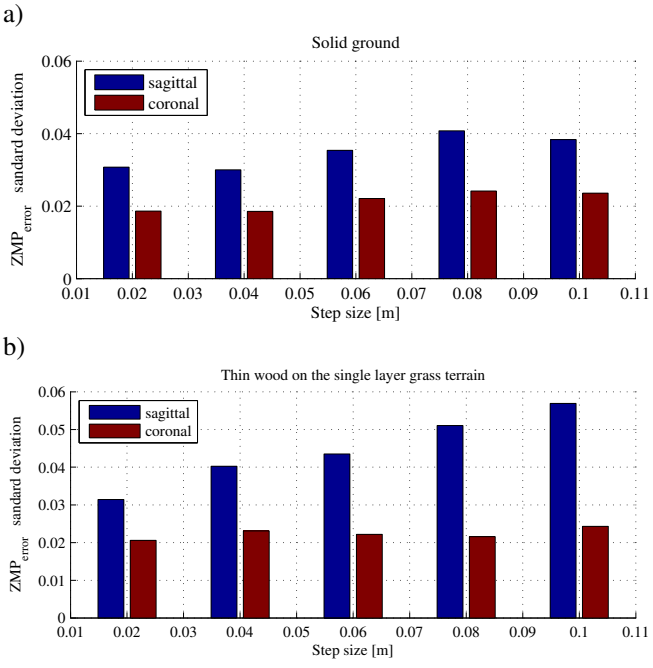

Fig. 6. Standard deviation of the ZMP error for the sagital and corronal plane for various terrains: a) terrain 1 (solid ground), b) terrain 5 (thin wood on the single layer grass). One can notice a clear correlation between the step size increase and error increase in terrain 5.

between the step size and the ZMP error standard deviation. The correlation matrix between the SD of the ZMP error in sagittal and coronal plane, and the step size for all the terrains is presented in Table I. A correlation between the

		Terrain type				
		1	2	3	4	5
Direction	Sagittal	0.88	0.77	0.96	0.95	0.99
	Coronal	0.91	-0.27	-0.18	0.97	0.65
Stab. Ind.		0.036	0.033	0.053	0.044	0.057

TABLE I

CORRELATION MATRIX AND FINAL STABILITY INDICATOR.

step size and the SD of the ZMP error on its own does not sufficiently reflect the stability of the locomotion, since it only indicates whether the SD of the ZMP increases with the step size. To solve that, we multiply the correlation value with the maximum SD value of the ZMP error, for a particular terrain and body plane. From the resultant values we choose the maximum one for the particular terrain and use it as an indicator of how the stability decreases when step size increase in particular terrain type. The bottom line in Table I contains the values for each of the terrain types. The higher the value is, the more unstable the system becomes when the step size increases. We can clearly see that the largest value is for the terrains number 3 (grass carpet) and 5 (wood on grass carpet), which coincides with the visual observation. In the further considerations we will denote as $\boldsymbol{s}$ the vector that contains these values.

D. Link Between Terrain Identification and Locomotion

Given that we are able to identify the terrain on which the locomotion takes place (Sec. III-B), we can use this information to optimise the locomotion stability and energy expenditure. The optimisation problem can be defined as follows:

$$\min_{i=1,..,5} F_t(i) \tag{3}$$

The objective is to find a step index i that will minimise the cost function F for the particular terrain t. The cost function components are the normalised step size dependent energy expenditure ${}^*\boldsymbol{e}$ and the terrain type dependent stability indicator ${}^*\boldsymbol{s}$. The normalisation is performed with respect to the maximum component of each vector.

$${}^*\boldsymbol{s}_t = \frac{\boldsymbol{s}_t}{max(\boldsymbol{s})}, for\ t = 1,..,5 \tag{4}$$

$${}^*\boldsymbol{e}_i = \frac{\boldsymbol{e}_i}{max(\boldsymbol{e})}, for\ i = 1,..,5$$

The cost function for each terrain t has the following form:

$$F_t(i) = K_E \cdot {}^*\boldsymbol{e}_i + K_S \cdot {}^*\boldsymbol{s}_t \cdot \boldsymbol{x}_i \tag{5}$$

where, K_E and K_S are weights of energy and stability components of the cost function, respectively.

	2 cm	4 cm	6 cm	8 cm	10 cm
	Fast Fourier Transform				
precision	81.49%	90.96%	84.00%	80.10%	74.95%
recall	80.00%	90.00%	82.00%	76.00%	76.00%
	Discrete Wavelet Transform				
precision	90.55%	86.11%	77.50%	84.05%	89.14%
recall	87.50%	85.00%	77.50%	82.50%	86.00%

TABLE II

CLASSIFICATION RESULTS FOR DIFFERENT STEP SIZES.

IV. RESULTS

Having described in detail the classification methodology along with the locomotion energy and stability analysis, we now present the results for each one of them. We then conclude with a discussion on the gait (i.e. step size) adaptation, based on the classification and the locomotion performance analysis.

A. Classification Results

Following the procedure described in Sec. III-B, we present and compare two classification approaches. The first one assumes that for each step size, a separate classifier will be used. For the testing set, the precision and recall results of this approach are presented in Table II. For the FFT case, the worst classification result is obtained for the largest step size and the best one for the 4cm step length. For the DWT case, the worst classification result is obtained for the 6cm step size and the best one for the 2cm step length. The obtained results of 82.30% mean precision and 80.80% mean recall for the FFT approach, as well as the 85.47% mean precision and 83.70% mean recall for the DWT approach, are close to the state-of-the-art in terms of tactile terrain identification. These values could be related to the results obtained for a six-legged robot [23], where the precision is 86.11% and the recall 90.70% (for 12 terrains), as well as for a quadruped robot [24], where the precision is 87.07% and the recall 86.81% (for 11 terrain types).

For the second approach, the feature vectors for all the step sizes were included in a single learning set (i.e. 600 steps), while the rest were used for the testing set (i.e. 200 steps), for which we used four-fold cross-validation. The obtained results for this procedure are as follows. The mean precision is $91.01 \pm 1.94\%$ and the mean recall is $90.75 \pm 1.94\%$ for the FFT approach, while the mean precision is $95.16 \pm 0.80\%$ and the mean recall is $95.00 \pm 0.82\%$ for the DWT approach. Following the second approach leads to an significant increase in the classification rates compared to the previous one, reaching very high precision and recall values. Moreover, the results for the DWT approach are better than the state-of-the-art ones (even though different F/T units, robots (2 vs 4/6 legs), and terrains were used in each work). The confusion matrix for the selected test data is shown in Fig. 7.

Further analysis of the results is given in Table III. It can be observed that the most challenging terrain for the FFT approach is the artificial grass carpet (terrain 3), while the one that is easily recognisable is the solid ground (terrain 1).

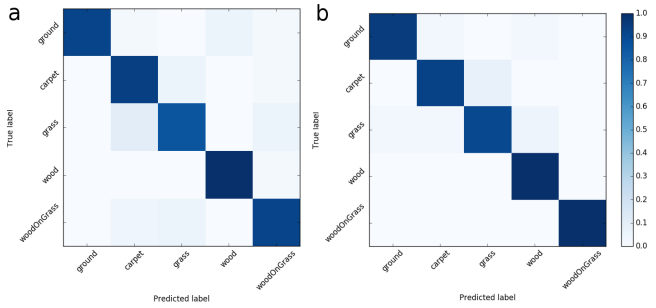

Fig. 7. Confusion matrix for all terrains and step sizes used in a single learning process based on: FFT features (a) and DWT features (b).

	ground	carpet	grass	wood	woodOnGrass
	Fast Fourier Transform				
precision	100.00%	85.19%	87.50%	94.23%	88.24%
recall	90.00%	92.00%	84.00%	98.00%	90.00%
	Discrete Wavelet Transform				
precision	97.56%	95.12%	92.68%	93.33%	100.00%
recall	95.24%	92.86%	90.48%	100.00%	100.00%

TABLE III

CLASSIFICATION RESULTS FOR EACH CLASS SEPARATELY.

For the DWT approach the performance for terrain 5 is the best and for terrain 3, similarly to the FFT, is the worst.

B. Stability & Energy Results

Using the cost function in Eq. (5), described in Sec. III-D, we can tune the weights to balance between the energy and stability of locomotion on various terrains. Fig. 8 shows the cost function values for all of the five terrains, for three different combinations of the K_E/K_S ratio. The high ratio prioritises the energy consumption by increasing the cost with the step decrease, while the lowest ratio prioritises the stability of locomotion by increasing the cost for bigger steps. We can see that the latter increase in the cost function, due to the increase in the step size, depends on the stability indicator $\boldsymbol{s}$. We noticed that $K_E = 2.5$ and $K_S = 10$ weights give a reasonable trade off between the two factors. For these weights, the resultant step size was 0.1m for the terrains 1, 2, and 4 and 0.06m for terrains 3 and 5. For this combination of step sizes the maximum SD of the ZMP is below 0.047m and the energy expenditure of walking for a distance of 0.5m is below 1084J. To compare, for $K_S = 2$, for all the terrain types, the optimal step size is 0.1m, giving the best energy efficiency, but the worst stability. On the other hand, for $K_S = 40$, the optimal step size for all the terrain types is 0.04m, which is thus optimising the stability, but not the energy efficiency.

C. Discussion of the Results

From the locomotion point of view we provided a tool that let us quantify the stability of locomotion on various types of terrains in an easy way and later use it to select gait parameters (in our case it is the step size) that optimise at the same time both the energy and the stability of the

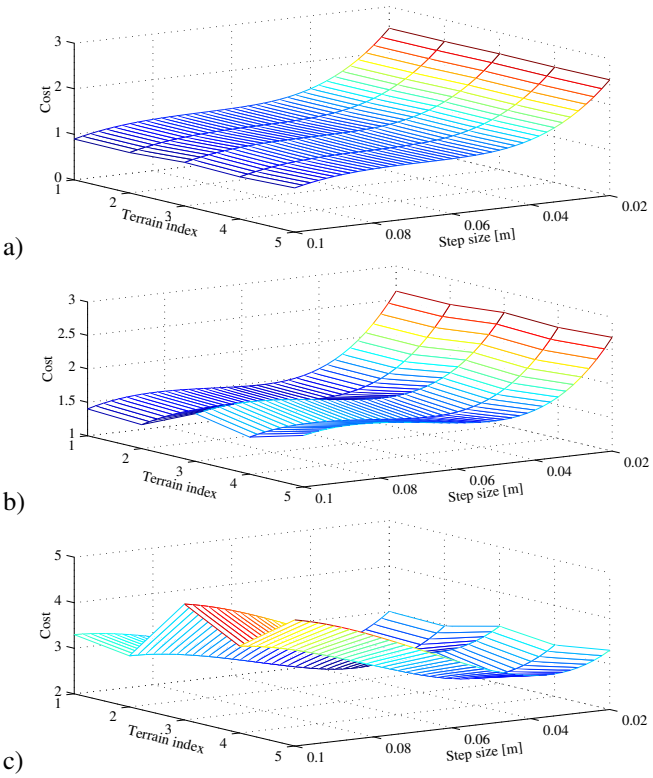

Fig. 8. Comparison of cost functions for all five terrains for different sets of K_E and K_S weights. In all the graphs $K_E = 2.5$, while the ratios K_E/K_S are: a) 1.25, b) 0.25 and c) 0.06.

locomotion. The two weights of the cost function provide a simple way to tweak the importance of the two factors.

Unfortunately, because of the lack of a robot state estimator, we were not able to analyse the CoM trajectory, which perhaps could be a better indicator of the long term locomotion stability. We are leaving this as a future work.

From the terrain identification point of view we were able to provide reliable results with high classification ratio, which surpass the state-of-the-art methods for different walking platforms, but on a smaller set of terrains. The boost of performance, when using data for all step sizes in one large learning set, is noticeable. The possible explanation to this fact is that the machine learning algorithm (SVM) has more data and provide better separation of the classes.

Dependable classification results provide the locomotion controller with the information needed for stable, yet energy efficient locomotion. In our work, unlike other approaches such as in [2], [10], [11], [12] where the terrain type was assumed, we are providing this information to the system.

V. CONCLUSIONS

In this paper, we first proposed an accurate terrain classification method, which outperforms the state-of-the-art approaches. It uses SVM learning to identify the type of a terrain, based on force/torque data acquired from the robot's ankle sensors and a signal descriptor formed using the Discrete Wavelet Transform approach. For each terrain type

and step size we performed a locomotion energy/stability analysis to identify the right step size for each terrain that balances the energy expenditure and the locomotion stability.

The work presented in this paper is a first approach to the longer research effort focused on two crucial aspects of robotic locomotion:

- To identify on-line ground mechanical properties, such as stiffness and damping.
- To modulate in real-time the gains of the ankle admittance and the ZMP stabilising controller, based on the identified mechanical properties of the terrain. This will allow the robot to accommodate with big changes in the ground properties and walk on much broader range of terrains.

On the other hand, inspired by the very good classification results from F/T sensor signals we plan to extend this work to a broader set of terrain types, including more challenging ones, such as sandy or rocky ones. Moreover, the visual range or lidar sensing will be used together with the F/T readings. The focus will be on a further improvement of the terrain classification methods, inluding data fusion techniques. Last but not least, other types of gait adaptation will be considered, such as the stiffness of the active compliant joints.

ACKNOWLEDGMENT

This work is supported by the European Union Seventh Framework Programme FP7-ICT-2013-10 under grant agreement no 611832 (WALK-MAN) and the ECs Horizon 2020 robotics program ICT-23-2014 under grant agreement 644727 (CogIMon). K. Walas is supported by the Poznań University of Technology grant DSPB/0148-2016 and DSMK/0154-2016.

REFERENCES

[1] DRC-Teams, "What Happened at the DARPA Robotics Challenge?" www.cs.cmu.edu/ cga/drc/events, 2015.

[2] M. Hopkins, R. Griffin, A. Leonessa, B. Lattimer, and T. Furukawa, "Design of a Compliant Bipedal Walking Controller for the DARPA Robotics Challenge," in *IEEE-RAS 15th Int. Conf. on Humanoid Robots (Humanoids)*, Nov 2015, pp. 831–837.

[3] Y. Ito *et al.*, "Development and verification of life-size humanoid with high-output actuation system," in *IEEE Int. Conf. on Robotics and Automation (ICRA)*, May 2014, pp. 3433–3438.

[4] N. A. Radford *et al.*, "Valkyrie: NASA's First Bipedal Humanoid Robot," *Journal of Field Robotics*, vol. 32, no. 3, pp. 397–419, 2015.

[5] N. G. Tsagarakis *et al.*, "WALK-MAN: A High Performance Humanoid Platform for Realistic Environments," *Journal of Field Robotics (JFR)*, 2016.

[6] S. Kajita, F. Kanehiro, K. Kaneko, K. Fujiwara, and K. H. K. Yokoi, "Biped Walking Pattern Generation by Using Preview Control of Zero-Moment Point," in *IEEE Int. Conf. on Robotics and Automation (ICRA)*, 2003, pp. 1620–1626.

[7] J. Lim, I. Shim, O. Sim, H. Joe, I. Kim, J. Lee, and J.-H. Oh, "Robotic Software System for the Disaster Circumstances: System of team KAIST in the DARPA Robotics Challenge Finals," in *IEEE-RAS 15th Int. Conf. on Humanoid Robots (Humanoids)*, Nov 2015, pp. 1161–1166.

[8] S. Nozawa *et al.*, "Multi-Layered Real-Time Controllers for Humanoid's Manipulation and Locomotion Tasks with Emergency Stop," in *IEEE-RAS 15th Int. Conf. on Humanoid Robots (Humanoids)*, Nov 2015, pp. 381–388.

[9] S. Kuindersma, F. Permenter, and R. Tedrake, "An Efficiently Solvable Quadratic Program for Stabilizing Dynamic Locomotion," in *IEEE Int. Conf. on Robotics and Automation (ICRA)*, May 2014.

[10] S. Kim *et al.*, "Approach of Team SNU to the DARPA Robotics Challenge Finals," in *IEEE-RAS 15th Int. Conf. on Humanoid Robots (Humanoids)*, Nov 2015, pp. 777–784.

[11] K. Hashimoto *et al.*, "Realization of Biped Walking on Soft Ground with Stabilization Control Based on Gait Analysis," in *Intelligent Robots and Systems (IROS), 2012 IEEE/RSJ Int. Conf. on*, 2012, pp. 2064–2069.

[12] M. Brandao, K. Hashimoto, J. Santos-Victor, and A. Takanishi, "Optimizing Energy Consumption and Preventing Slips at the Footstep Planning Level," in *Humanoid Robots (Humanoids), 2015 IEEE-RAS 15th Int. Conf. on*, Nov 2015, pp. 1–7.

[13] D. Kanoulas and M. Vona, "Bio-Inspired Rough Terrain Contact Patch Perception," in *Proceedings of the IEEE Int. Conf. on Robotics and Automation (ICRA)*, 2014.

[14] D. Kanoulas, "Curved Surface Patches for Rough Terrain Perception," Ph.D. dissertation, CCIS, Northeastern University, August 2014.

[15] C. Kertesz, "Rigidity-Based Surface Recognition for a Domestic Legged Robot," *IEEE Robotics and Automation Letters*, vol. 1, no. 1, pp. 309–315, Jan 2016.

[16] M. Hoffmann, K. Stepanova, and M. Reinstein, "The Effect of Motor Action and Different Sensory Modalities on Terrain Classification in a Quadruped Robot Running with Multiple Gaits," *PRobotics and Autonomous Systems*, vol. 62, no. 12, pp. 1790–1798, 2014.

[17] J. Mrva and J. Faigl, "Feature Extraction for Terrain Classification with Crawling Robots," in *Proceedings ITAT 2015: Information Technologies - Applications and Theory, Slovensky Raj, Slovakia, September 17-21, 2015.*, 2015, pp. 179–185.

[18] P. Dallaire, K. Walas, P. Giguere, and B. Chaib-draa, "Learning Terrain Types with the Pitman-Yor Process Mixtures of Gaussians for a Legged Robot," in *IEEE/RSJ Int. Conf. on Intelligent Robots and Systems (IROS)*, Sept 2015, pp. 3457–3463.

[19] L. Ding, H. Gao, Z. Deng, J. Song, Y. Liu, G. Liu, and K. Iagnemma, "Foot–Terrain Interaction Mechanics for Legged Robots: Modeling and Experimental Validation," *The Int. J. of Robotics Research*, vol. 32, no. 13, pp. 1585–1606, 2013.

[20] P. Filitchkin and K. Byl, "Feature-Based Terrain Classification for LittleDog," in *IEEE/RSJ Int. Conf. on Intelligent Robots and Systems (IROS)*, 2012, pp. 1387–1392.

[21] S. Namin and L. Petersson, "Classification of Materials in Natural Scenes Using Multi-Spectral Images," in *IEEE/RSJ Int. Conf. on Intelligent Robots and Systems (IROS)*, Oct 2012, pp. 1393–1398.

[22] K. Walas and M. Nowicki, "Terrain Classification using Laser Range Finder," in *IEEE/RSJ Int. Conf. on Intelligent Robots and Systems (IROS)*, 2014, pp. 5003–5009.

[23] K. Walas, "Terrain Classification and Negotiation with a Walking Robot," *Journal of Intelligent & Robotic Systems*, vol. 78, no. 3-4, pp. 401–423, 2015.

[24] M. Höpflinger *et al.*, "Haptic Terrain Classification for Legged Robots," in *IEEE Int. Conf. on Robotics and Automation (ICRA)*, 2010, pp. 2828–2833.

[25] G. Metta, P. Fitzpatrick, and L. Natale, "YARP: Yet Another Robot Platform," *Int. Journal on Adv. Robotics Syst.*, vol. 3, no. 1, 2006.

[26] M. Quigley *et al.*, "ROS: an open-source Robot Operating System," in *ICRA Workshop on Open Source Software*, 2009.

[27] K. Nagasaka, M. Inaba, and H. Inoue, "Stabilization of Dynamic Walk on a Humanoid using Torso Position Compliance Control (in Japanese)," in *Proceedings of 17th Annual Conf. of the Robotics Society of Japan*, 1999, pp. 1193–1194.

[28] I. Daubechies, *Ten Lectures on Wavelets*. Society for Industrial and Applied Mathematics, 1992.

[29] C.-C. Chang and C.-J. Lin, "LIBSVM: A Library for Support Vector Machines," *ACM Trans. on Intelligent Systems and Technology*, vol. 2, pp. 27:1–27:27, 2011, software available at http://www.csie.ntu.edu.tw/ cjlin/libsvm.

[30] K. Walas, M. Czachorowski, and T. Halasz, *Influence of Walking Speed and Direction of Movement on Tactile Ground Classification Process*. World Scientific, 2014, ch. 69, pp. 591–599.

[31] N. Koenig and A. Howard, "Design and Use Paradigms for Gazebo, An Open-Source Multi-Robot Simulator," in *IEEE/RSJ Int. Conf. on Intelligent Robots and Systems (IROS)*, Sendai, Japan, Sep 2004, pp. 2149–2154.